Title: Competitive sorption of Pb(II), Cu(II) and Ni(II) on carbonaceous nanofibers: a spectroscopic and modeling approach

Author: Congcong Ding Wencai Cheng Xiangxue Wang Zhen-Yu Wu Yubing Sun Changlun Chen Xiangke Wang Shu-Hong Yu

PII: S0304-3894(16)30332-6
DOI: http://dx.doi.org/doi:10.1016/j.jhazmat.2016.04.002
Reference: HAZMAT 17610

To appear in: *Journal of Hazardous Materials*

Received date: 17-12-2015
Revised date: 27-3-2016
Accepted date: 3-4-2016

Please cite this article as: Congcong Ding, Wencai Cheng, Xiangxue Wang, Zhen-Yu Wu, Yubing Sun, Changlun Chen, Xiangke Wang, Shu-Hong Yu, Competitive sorption of Pb(II), Cu(II) and Ni(II) on carbonaceous nanofibers: a spectroscopic and modeling approach, Journal of Hazardous Materials http://dx.doi.org/10.1016/j.jhazmat.2016.04.002

Competitive sorption of Pb(II), Cu(II) and Ni(II) on carbonaceous nanofibers: a spectroscopic and modeling approach

Congcong Ding [†,‡,§], Wencai Cheng [†,‡,§], Xiangxue Wang[†,‡,§], Zhen-Yu Wu[#], Yubing Sun [‡]*, Changlun Chen[‡]*, Xiangke Wang [†,∥,⊥]*, Shu-Hong Yu[#]

† School of Environment and Chemical Engineering, North China Electric Power University, Beijing 102206, P. R. China

‡ Key Lab of New Thin Film Solar Cells, Institute of Plasma Physics, Chinese Academy of Science, P.O. Box 1126, Hefei, 230031, P.R. China

§ University of Science and Technology of China, Hefei, 230032, P.R. China

∥ Collaborative Innovation Center of Radiation Medicine of Jiangsu Higher Education Institutions and School for Radiological and Interdisciplinary Sciences, Soochow University, 215123, Suzhou, P.R. China

⊥ NAAM Research Group, Faculty of Science, King Abdulaziz University, Jeddah 21589, Saudi Arabia

 # Division of Nanomaterials and Chemistry, Hefei National Laboratory for Physical Science at Microscale, Department of Chemistry, University of Science and Technology of China, Hefei, Anhui 230026.

Graphical Abstract

Higher affinity of CNFs for Pb(II) than Ni(II) and Cu(II)

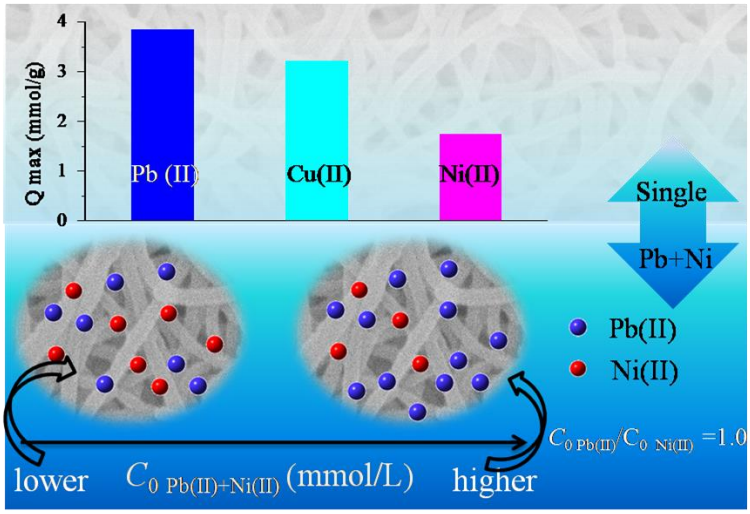

Highlights

- Inner-sphere complexation dominated sorption Pb(II), Cu(II) and Ni(II) on CNFs.
- Pb(II) exhibited greater inhibition of the sorption of Cu(II) and Ni(II) on CNFs.
- Competitive sorption was predicted quite well by surface complexation modeling.
- Sorption of heavy metals on CNFs were covalent bonding by EXAFS analyses.

Abstract

The competitive sorption of Pb(II), Cu(II) and Ni(II) on the uniform carbonaceous nanofibers (CNFs) was investigated in binary/ternary-metal systems. The pH-dependent sorption of Pb(II), Cu(II) and Ni(II) on CNFs was independent of ionic strength, indicating that inner-sphere surface complexation dominated sorption Pb(II), Cu(II) and Ni(II) on CNFs. The maximum sorption capacities of Pb(II), Cu(II) and Ni(II) on CNFs in single-metal systems at a pH 5.5 ± 0.2 and 25 ± 1 °C were 3.84 (795.65 mg/g), 3.21 (204.00 mg/g) and 2.67 (156.70 mg/g) mmol/g, respectively. In equimolar binary/ternary-metal systems, Pb(II) exhibited greater inhibition of the sorption of Cu(II) and Ni(II), demonstrating the stronger affinity of CNFs for Pb(II). The competitive sorption of heavy metals in ternary-metal systems was predicted quite well by surface complexation modeling derived from single-metal data. According to FTIR, XPS and EXAFS analyses, Pb(II), Cu(II) and Ni(II) were specifically adsorbed on CNFs via covalent bonding. These observations should provide an essential start in simultaneous removal of multiple heavy metals from aquatic environments by CNFs, and open the doorways for the application of CNFs.

Key words: carbonaceous nanofibers; competitive sorption; heavy metals; EXAFS analysis; surface complexation modeling.

1. Introduction

Various heavy metals are expected to mostly coexist in aquatic environments as a result of various activities such as hydrogeological, volcanic and anthropogenic activity. For example, zinc and lead would be simultaneously discharged into the environment during the mining and milling of copper mine [1]. Such coexisting heavy metals cause deleterious effects on humans and other organisms even at low exposure levels [2]. Thus, the remediation of coexisting heavy metals in water supplies has become an increasingly public and environmental concern in developing and industrialized countries [3]. The simultaneous sorption of various heavy metals on a variety of adsorbents has been extensively investigated in recent years [4-8]. Although the high sorption capacities of these adsorbents were reported in these studies, more attention concerning co-adsorption mechanism of various heavy metals by combing spectroscopic and modeling techniques was not available.

Recently, carbonaceous nanofibers (CNFs) have been produced via hydrothermal carbonization (HTC) by using glucose as the precursor [9]. The CNFs obtained from this method exhibit the excellent mechanical stability, large surface area, and good hydrophilic nature [10]. CNFs have attracted much research interest for the construction of 2D macroscopic membranes that have significant potential applications in many fields such as optoelectronic devices [11], gas sensors [12], and filters for gas and water treatment [13]. A fabricated CNF membrane was confirmed to exhibit efficient size-selective filtration and separation of nanoparticles from water due to the controllable diameter, narrow size distribution and high uniformity of the CNFs [14]. Wu et al. [15] also reported that CNF aerogels displayed a high sorption capacity for the cleanup of oil spillage and chemical leakage. Considering the good performance of CNF membranes in water filtration, CNFs should have potential for the concurrent preconcentration of heavy metal ions due to their abundant oxygen-containing groups (i.e., -OH and -COOH groups), the large surface area and their environmentally friendly nature [9]. Additionally, HTC is also a green and economic chemistry process [14]. Besides, our recent studies revealed that the synthetic of CNFs could be enlarged to 1200 mL in one pot, which indicates the

possibility of industrial production of CNFs [10]. However, the mechanism of interaction of CNFs with heavy metal ions has not yet been well described [10], especially in heterogeneous aquatic environments. The identification of the molecular-level interaction mechanisms between CNFs and heavy metal ions remains challenging in multi-metal systems because of the limitations of currently available data and spectroscopic signatures.

Extended X-ray absorption fine structure (EXAFS) spectroscopy and surface complexation modeling (SCM) have been extensively used as powerful tools for the interpretation of the interaction mechanism between adsorbate and adsorbent [16-19]. Based on EXAFS spectra, Strathmann et al. [20] demonstrated the formation of inner-sphere surface complexes of Ni(II) on short-chain dicarboxylates in oxalate and malonate, and carboxylates in actate, malate and citrate. Various SCMs such as the constant capacitance model (CCM) and the double diffuse model (DLM) have shown encouraging success at describing metal sorption on adsorbents in single and competitive systems [21-23]. Sun et al. [18] used SCMs to satisfactorily fit the sorption of U(VI) on graphene oxides with strong (SsOH) and weak (SwOH) sites. Hence, the use of EXAFS and SCM analysis is necessary to develop a thorough understanding of the molecular-level sorption mechanisms which help accurately evaluate the fate and transport of heavy metals in natural aquatic systems.

In this study, Pb(II), Cu(II) and Ni(II) have been chosen as representative of heavy metals since they are toxic to organisms even at low concentrations and are among the most common pollutants found in industrial effluents [4]. For example, lead can damage the nervous and reproductive systems, whereas nickel can cause lung and nasal sinus cancers [4]. The objectives of this study are to (1) investigate the individual and competitive sorption of Pb(II), Cu(II) and Ni(II) on CNFs at different pH values and different initial concentrations; (2) explore the interaction mechanism between CNFs and heavy metals using EXAFS, X-ray photoelectron spectroscopy (XPS), Fourier transformed infrared (FTIR) spectroscopy, and SCMs. The highlights of this study are the identification of the sorption and desorption nature of CNFs toward multi-species of heavy metals and the relevant mechanisms, which is expected

to provide some meaningful information about CNFs for further engineering application in heavy metal treatments.

2. Materials and methods

2.1. Materials

CNFs were prepared by a template-directed hydrothermal carbonization process according to previous reports [9, 14, 24]. Typically, 30 mL of acetone was added to 10 mL of the prepared tellurium (Te) nanowires to precipitate the product before centrifuging at 6000 rpm. Then, the Te products were dispersed into 80 mL of 62.5 g/L glucose solution under vigorous magnetic stirring for 15 min. The well-defined Te/C nanocables were obtained after hydrothermal treatment of the mixed solution at 160 ºC for 36 h. Pure CNFs could be obtained by chemical etching in mixing solutions of HCl and H_2O_2 (HCl: H_2O_2: H_2O = 2: 5: 23, v/v) to remove Te cores (see the Supporting Information (*SI*) for details). It should be pointed out that the template-directed synthesis is a generalized method since Te nanowires could be replaced by other inexpensive nanowires [14]. Additionally, Te nanowires could be recycled and converted to TeO_3^{2-} again during fabrication process [10]. The element analysis of as-prepared CNFs was recorded by Elementar Vario EL-III (Germany), which revealed that CNFs contained 70.0 wt % C, 6.4 wt % H and 23.6% O. Other element was not detectable, suggesting no detectable impurities of CNFs. The specific surface area of CNFs measured by N_2-BET analysis was 150.3 m^2 g^{-1} using Micromeritics Gemini II 2375.

1 mmol/L stock solutions of Pb(II) (207.20 mg/L), Cu(II) (63.55 mg/L) and Ni(II) (58.69 mg/L) were prepared by dissolving $Pb(NO_3)_2$, $Cu(NO_3)_2{\cdot}3H_2O$ and $Ni(NO_3)_2{\cdot}6H_2O$ (99.9% purity, Sigma-Aldrich, USA) in 1.0 mmol/L HNO_3 solution, respectively. All other reagents of analytical grade were purchased from Sinopharm Chemical Reagent Co., Ltd., Shanghai, China, and were used directly without further purification.

2.2. Bath sorption and desorption experiment

Batch sorption experiment was conducted with 0.2 g/L CNFs and 0.2 mmol/L heavy metal solution at T = 25 ± 1 °C in the presence of 0.001, 0.01 or 0.1 mol/L $NaClO_4$

solutions. Because ClO_4^- has little capacity to coordinate with metal ions [25], $NaClO_4$ would not affect Pb(II), Cu(II) and Ni(II) species with varied pH and would contribute to the mechanistic description of heavy metal sorption on CNFs. Briefly, the bulk suspensions of CNFs and $NaClO_4$ were pre-equilibrated for 24 h in closed polycarbonate tubes, and then the metal stock solution was spiked into the bulk suspensions. In order to near the neutral pH values of environment and avoid the precipitation of heavy metals at alkaline pH, all the experiments were conducted at pH 5.5 ± 0.2 unless pH was varied. For *pH effect* portion, the pH value was adjusted to be in the range of 3.5-9.5 ± 0.2 for single-metal system, and of 3.5-9.0 ± 0.2 for ternary-metal (Pb-Cu-Ni) system by adding a negligible volume of 0.01-1.00 mol/L NaOH and $HClO_4$. The sorption isotherms of Pb(II), Cu(II) and Ni(II) were investigated with concentration ranging from 0.1 to 0.6 mmol/L in 0.001 mol/L $NaClO_4$ solutions. Competitive sorption of heavy metals on CNFs was conducted in binary/ternary-metal systems with equivalent concentrations of each metal. After equilibrium, the suspension was centrifuged at 9000 rpm for 10 min and then filtered through a 0.45 μm nylon membrane filter. The concentrations of heavy metal ions in the supernatant were measured by an inductively-coupled plasma-atomic emission spectrometer (ICP-AES, CAP6300, Thermo Scientific). These data were used to calculate the sorption percentage (sorption (%)) and sorption capacity (Q (mmol/g)). The details for the sorption experiments are described in the *SI*.

The desorption experiments of Pb(II), Cu(II) and Ni(II) were conducted after their equilibrium of sorption isotherms in single-metal system. After centrifuging, a half volume of the supernatant was displaced by the equivalent volume of sorbate-free (Pb(II)-, Cu(II)- and Ni(II)-free) background electrolyte solution with the same pH values. After the equilibrium of the suspension, the supernatants were measured to calculate the residual concentrations of heavy metals on CNFs by mass balance.

2.3. Characterization

CNFs, thus prepared, were characterized by scanning electron microscopy (SEM), transmission electron microscopy (TEM), XPS, potentiometric acid−base titration, and FTIR. The SEM and TEM images were obtained by a field emission scanning

electron microscope (FEI-JSM 6320F) and transmission electron microscope (JEM-2010, Japan), respectively. XPS data were acquired with a Thermo Escalab 250 XPS with Al Kα radiation at 150 W. The energies were corrected using the C 1s peak at 284.6 eV as a reference, and the data were analyzed using the XPSPEAK software (version 4.1). The potentiometric acid-base titration was performed to determine the chemical properties of CNFs by use an automatic titrator (DL50, Mettler Toledo). Titration experiment was conducted with 0.2 g/L CNFs in the presence of 0.001 mol/L $NaClO_4$ solution as the background electrolyte. The details are presented in *SI*. FTIR spectra of samples before and after sorption were obtained from a JASCO FTIR 410 spectrophotometer in the range of 4000-400 cm^{-1} using the KBr disc technique.

2.4. Surface Complexation Modeling

With the aid of the Visual MINTEQ program, the sorption of heavy metals on CNFs at 0.001 mol/L $NaClO_4$ solutions was simulated by using a CCM due to its simple format and few parameters [26]. CCM model assumes that a simple linear relationship exists between surface potential and the surface charge density through the capacitance [27]. According to a previous report [28], the inner-layer capacitance value for CNFs was chosen to be around 2.01 F/m^2. The surface acidity constants of the CNFs were obtained by fitting potentiometric titration data. The sorption constants (log *K*) for each metal were obtained by best fitting of the experimental data of heavy metals on CNFs. More details about the fitting process are provided in the *SI*.

2.5. EXAFS Analysis

Samples for EXAFS analysis were prepared in a manner similar to the preparation described for the sorption experiments. In this study, Ni(II) was chosen to be representative of the heavy metals to conduct the EXAFS analysis. After sorption equilibrium at different values of pH (5.5, 7.0 and 9.5), the suspensions of Ni(II) were centrifuged to obtain the wet pastes for EXAFS analysis. Ni K-edge EXAFS spectra were recorded at 8333 eV at the Shanghai Synchrotron Radiation Facility (SSRF, China) in fluorescence (sorption samples and Ni(II)(aq)) and transmission ($Ni(OH)_2(s)$) modes. The details for EXAFS preparation are listed in the *SI*.

3. Results and discussion

3.1. Characterization

The morphology and nanostructure of CNFs were characterized by SEM and TEM. An interconnected 3D framework of CNFs with many junctions is shown in Fig. 1A. It can be observed that CNFs exhibit a surprisingly high uniformity and a narrow diameter size distribution of ca. 100 nm. The high resolution of TEM image reveals the smooth surface of CNFs, and no hollow is observed in CNFs surfaces (Fig. 1B). The high-resolution C1s XPS spectrum of CNFs and its deconvolution are shown in Fig. 1C. The C 1s spectra can be fitted by C-C/C-H at 284.7 eV, C-O at 286.4 eV, C=O/O-C-O at 288.0 eV, and O-C=O at 289.0 eV [29], suggesting the presence of variety of oxygenated functional groups in CNFs. The oxygenated groups of CNFs were further evidenced by the analysis of FTIR (Fig. 4) and O 1s XPS spectra (Fig. S1 in *SI*). The formation of abundant oxygenated groups in CNFs could result from the incomplete carbonization of glucose at temperatures as low as 160 ºC [9]. These oxygenated functional groups are not only able to increase the hydrophilicity of CNFs, but can also provide abundant reactive sites for the sorption of heavy metals. Based on the determination of potentiometric acid-base titration in Fig. 1D, the pH_{PZC} (pH at point of zero charge) value of CNFs was 4.4.

3.2. Effect of pH and ionic strength

Figure 2A-C show the effect of pH on the sorption of Pb(II), Cu(II) and Ni(II) on CNFs in single-metal system. The sorption of Pb(II), Cu(II) and Ni(II) on CNFs in single-metal system increased with increasing pH from 3.0 to 7.0, and a plateau (~ 100% metal sorption) was observed at pH > 8.0, which is similar with the sorption trend of other reported adsorbents toward these metals [4, 22]. However, Anna et al. [5] reported the maximum sorption of Pb(II) and Cu(II) on natural bentonite at pH 5.0. It should be pointed out that the dependence of metal uptake on pH is related to both the surface functional groups of adsorbents and the metal chemistry in solution [17]. Besides, the experimental conditions like concentrations of adsorbent and metals also affect the sorption trend. The shift of the Pb(II) sorption edge to a lower pH relative to Cu(II) and Ni(II) suggested the greater affinity of CNFs for Pb(II). The effect of ionic

strength on the sorption of Pb(II), Cu(II) and Ni(II) on CNFs at single-metal system is also shown in Fig. 2A-C. The ionic strength can influence the electric double layer thickness and interface potential [17, 30], thus affecting the electrostatic attraction between heavy metals and CNFs. Outer-sphere surface complexation (i.e., electrostatic interaction) was expected to be more sensitive to the ionic strength variations, whereas inner-sphere surface complexation with covalent bonding was not dependent on the ionic strength [30-32]. As shown in Fig. 2A-C, the ionic strength-independent sorption of Pb(II), Cu(II) and Ni(II) on CNFs in single-metal system indicated that inner-sphere surface complexation dominated their sorption. Besides, the competitive sorption of Pb(II), Cu(II) and Ni(II) on CNFs in binary-metal system was also little influence by the ionic strength (Fig. S4). Thus, the increased sorption of Pb(II), Cu(II) and Ni(II) with increasing pH could be attributed to the enhanced ability of deprotonation of oxygenated groups in CNFs which were more readily to coordinate with the metallic or hydrolyzed metallic cations (i.e., Pb^{2+} or $Pb(OH)^{+}$). Additionally, the precipitation/coprecipitation of Pb(II), Cu(II) and Ni(II) as shown in Fig. S2 probably accounted for the high sorption at pH > 7.0.

Fig. 2D shows the competitive sorption of metals in a ternary Pb-Cu-Ni system as a function of pH, which is similar to the pH effect in a single-metal system. Pb(II) sorption on CNFs was slightly affected by Cu(II) and Ni(II) cations over pH 3.0-7.0, whereas the existence of Pb(II) significantly inhibited the sorption of Cu(II) and Ni(II), further demonstrating the higher affinity of Pb(II) for CNFs. For example, approximately 60 % and 20 % of Ni(II) were adsorbed to CNFs in the single-metal and Pb-Cu-Ni systems, respectively, at pH 5.5. However, the inhibition effect at pH > 7.0 and pH > 8.0 was not obvious for Cu(II) and Ni(II), respectively, which might result from the precipitation of Cu(II) and Ni(II) on CNFs.

3.3. Surface complexation modeling

The pH-dependent sorption data of Pb(II), Cu(II) and Ni(II) on CNFs in single-metal system in 0.001 mol/L $NaClO_4$ were fitted by CCM model with the aid of the Visual MINTEQ program [26]. The fitting results and surface species distribution of each metal are represented as lines in Fig. 2A-C. The model can describe the experimental

data reasonably well. As shown in Fig. 2A-C, the sorption of Pb(II), Cu(II) and Ni(II) on CNFs can be well fitted by ≡SOM$^+$ and ≡SOMOH species at lower and higher pH, respectively (M^{2+} refers to Pb(II), Cu(II), and Ni(II) cations). The addition of ≡SO$Cu_3(OH)_4^+$ species at higher pH was needed to fit the Cu(II) sorption on CNFs well, which might be related to the distribution of Cu species in aqueous solutions. The optimized fitting parameters are summarized in Table 1, and the results demonstrated that the sorption constant (log $K_{(\equiv SOM+)}$) of Pb(II) on CNFs (-0.45) was higher than the sorption constant of Cu(II) (-0.79) and Ni(II) (-0.96), further demonstrating the higher affinity of CNFs for Pb(II). According to previous reports, a multi-metallic sorption process can be predicted on the basis of a combination of simple single-metal sorption reactions [21]. Thus, the optimized model parameters were further validated by predicting the competitive sorption of heavy metals in ternary Pb-Cu-Ni system. The competitive sorption of Pb(II), Cu(II) and Ni(II) in Fig. 2D was simulated by combinations of individual sorption reactions and their sorption constants fitted in single-metal system (Table 1). As depicted in Fig. 2D, the model described the competition effects between these heavy metals well at pH < 7.5. However, the model tended to underestimate the sorption of Pb(II) and Cu(II) in a ternary-metal system at pH > 7.5. Reddad et al. [21] found that the competitive metal binding effects on natural polysaccharide can be well predicted by the SCMs over pH 2.0-5.5. The underestimation might result from the precipitation of heavy metals at a higher pH and the lack of consideration of other sorption sites on CNFs.

3.4. Sorption isotherms

Figure 3 shows the sorption isotherms of heavy metals on CNFs in single-metal and binary/ternary-metal systems. The sorption of heavy metals on CNFs in single-metal systems was significantly higher than in binary/ternary-metal systems, suggesting the presence of inhibition effects [33]. The corresponding maximum sorption capacities of Pb(II), Cu(II) and Ni(II) on CNFs were listed in Table 2-3. As shown in Fig. 3A, the inhibition of sorption of Ni(II) on CNFs in a Pb-Ni system was significantly higher than the inhibition of sorption in a Cu-Ni system. Similarly, the higher inhibition of sorption of Cu(II) was also observed in Pb-Cu system relative to Cu-Ni

system (Fig. 3B). These results suggested that Pb(II) showed a high inhibition effect on the sorption of Ni(II) and Cu(II) to CNFs. Thus, the decrease of Ni(II) and Cu(II) sorption in a Pb-Cu-Ni system might mainly result from that more reactive sites of CNFs were occupied by Pb(II) ions. However, the extent of the reduction of Pb(II) sorption in binary/ternary-metal systems was lower than the extent of the reduction of Ni(II) and Cu(II) sorption in binary/ternary-metal systems (Fig. 3C), suggesting a higher affinity of CNFs for Pb(II) [34]. The preferred sorption of Pb(II) on CNFs was supported by the maximum sorption capacities calculated by the Langmuir model (Table 2), which were 3.84 (795.65 mg/g), 3.21 (204.00 mg/g) and 2.67 (156.70 mg/g) mmol/g at pH 5.5 ± 0.2 in single-metal systems for Pb(II), Cu(II) and Ni(II), respectively. As shown in Table 3, the maximum sorption capacity in Pb-Cu-Ni system also followed the order of Pb(II) (2.27 mmol/g (470.34 mmg/g)) > Cu(II) (1.55 mmol/g (98.50 mg/g)) > Ni(II) (1.1 mmol/g (64.56 mmg/g)). Compared with other carbonaceous adsorbents (Table S2), CNFs exhibited a higher sorption capacity for heavy metals, which might be attributed to the stronger affinity of metals to the binding sites, especially the oxygenated functional groups as characterized by the XPS and FTIR analysis, of CNFs. Fig. S5 also shows the decreased sorption capacity of heavy metals in the presence of a 0.2 mmol/L competing ion (i.e., 1.75 mmol/g for Ni(II) in the presence of Pb(II)).

For the Pb-Ni system, the sorption of Ni(II) reached a maximum, and then decreased with increasing Ni(II) equilibrium solution concentration (Fig. 3A), while the sorption of Pb(II) increased with increasing Pb(II) equilibrium solution concentration (Fig. 3C). The competitive sorption results indicated that the adsorbed Ni(II) was more easily displaced by Pb(II) at higher concentrations. However, a similar decrease was not observed for Ni(II) in the presence of 0.2 mmol/L Pb(II) (Fig. S5). Thus, we deduced that the sorption sites of CNFs, available to both Ni(II) and Pb(II) at low concentrations, was occupied solely by Pb(II) with increasing Ni(II) and Pb(II) concentration [35], resulting in a decrease of Ni(II) sorption. A similar trend was also observed in the Pb-Cu system (Fig. 3B,C). However, CNFs presented a stronger chemical affinity for Cu(II) compared to Ni(II) in Cu-Ni system (Fig. 3A,B).

Therefore, the chemical affinity of CNFs toward heavy metals followed the sequence Pb(II) > Cu(II) > Ni(II), which relates with the preferential sorption of metal on CNFs [35, 36]. Generally, metals with a higher uptake capacity in single-metal systems show a greater inhibitory effect on the sorption of other metal ions in the binary/ternary-metal systems.

3.5. Desorption isotherms

The desorption isotherms of Pb(II), Cu(II) and Ni(II) from CNFs are shown in Fig. 3D-F. It can be observed that the desorption isotherms of Pb(II), Cu(II) and Ni(II) significantly deviated from their sorption isotherms, and more metals remained adsorbed in desorption curves than that in sorption curves, revealing the sorption-desorption hysteresis [37]. According to previous reports, desorption hysteresis could be attributed to the irreversible chemical reaction/binding between heavy metals and adsorbents. [17, 38-40]. Undabeytia et al. [38] determined that desorption hysteresis of Cu(II) on the edge sites of montmorillonite arose from the formation of Cu(II) inner-sphere complexes on the edge surfaces. Therefore, the sorption-desorption hysteresis phenomenon reveals that the sorption of Pb(II), Cu(II) and Ni(II) on CNFs is an irreversible process, which might be caused by the covalent bonding of these metals with CNFs.

3.6. FTIR and XPS analysis

The FTIR spectra of CNFs and heavy metal-containing CNFs are shown in Fig. 4. CNFs possess a variety of oxygenated functional groups such as –OH (at ~3424 cm^{-1}) [6, 41] and –COOH (including C=O and the accompanying C-O at 1711 and 1204 cm^{-1}, respectively) groups [29]. The band at 1643 cm^{-1} was assigned to the C=C group [6]. After sorption of Pb(II), Cu(II) and Ni(II), C=O stretching of protonated COOH groups in CNFs at 1711 cm^{-1} disappeared , whereas the intensities of peaks at ~1390 and ~1590 cm^{-1} increased, which might be caused by the symmetrical (1407 cm^{-1}) and asymmetrical (1582 cm^{-1}) stretching of carboxylate anion ($-COO^-$) [29]. The resultant shifting of the peaks suggested the complexation of these metals with $-COO^-$ group. The sharp peak at ~1390 cm^{-1} was probably due to the adsorbed NO_3^- on samples which originated from these metal nitrates (i.e., $Pb(NO_3)_2$, $Cu(NO_3)_2 \cdot 3H_2O$ and

$Ni(NO_3)_2 \cdot 6H_2O$) [42]. Additionally, the OH groups (~3424 cm^{-1}) shifted to the higher frequency for Pb(II) (3447 cm^{-1}), Cu(II) (3439 cm^{-1}) and Ni(II) (3442 cm^{-1}), indicative of participation of OH groups in cationic metal sorption.

Figure 5A shows XPS survey spectra of CNFs and CNFs after the sorption of Pb(II), Cu(II) and Ni(II). After sorption, the peaks of Pb 4f/4d/4p, Cu 3p/2p and Ni 2p were observed, indicating that the heavy metals were adsorbed on CNFs. The high resolution of heavy metal peaks is provided in Fig. S1. Fig. 5B shows the high resolution of the O 1s peaks. Compared with the CNFs, the binding energy of the O1 s of the CNFs after sorption was remarkably shifted to the lower binding energy for Pb(II), Cu(II) and Ni(II). The shift of binding energy of the O 1s peaks indicated the coordination of the metallic cations with the oxygenated groups of the CNFs [43], which was consistent with previous studies [17, 25, 44, 45]. These results supported the inner-sphere sorption of Cu(II), Pb(II) and Ni(II) on CNFs, and were consistent with the analysis of FTIR. The results from the XPS and FTIR spectra indicated that Pb(II), Cu(II) and Ni(II) were specifically adsorbed on CNFs via covalent bonding with oxygenated functional groups.

Different chemical affinity was observed in terms of batch experiment and surface complexation modeling, which might result from the preference of oxygenated functional groups. According to the analysis of the O 1s XPS spectra, the shift degree of the O 1s peak for Pb(II) (1.5 eV) was more than the shift degree of O 1s peak for Cu(II) (0.9 eV) and Ni(II) (0.7 eV) (Table S1). The chemical affinity of CNFs for heavy metals was correlated with the chemical properties of the heavy metals such as electronegativity and first hydrolysis constants (log K_{MOH}) [33, 34, 46]. The values of log K_{MOH} were found to be ranked in the sequence of Pb(II) (-7.49)> Cu(II) (-7.59) > Ni(II) (-9.89) [34, 46]. Gu et al. [46] demonstrated that higher log K_{MeOH} values exhibited greater sorption ability. Thus, Pb(II) was preferentially adsorbed on CNFs due to the easier association with the oxygenated functional groups on CNFs than Cu(II) and Ni(II) [33], consistent with the results of surface complexation modeling.

3.6. EXAFS analysis

Figure 6 shows k^3-weighted Ni K-edge EXAFS spectra and the corresponding Fourier

transforms (FT, uncorrected phase shift) of the Ni(II) sorption samples and the reference standard (including Ni(II)(aq) and $Ni(OH)_2$(s)). The fitted results are also shown in Fig. 6 (dashed lines), and the corresponding fitted parameters are listed in Table S3. As shown in Fig. 6A, Ni(II) aqueous species exhibited only a single wave frequency of monotonically decreasing amplitude for $k > 3$ Å, suggesting that a single ordered coordination sphere was present. This observation is supported by the corresponding FT spectra (Fig. 6B). Only a single peak at ~ 1.6 Å was caused by the Ni-O backscattering [8, 47]. As shown in Table S3, the first shell can be fitted ~ 6 O at an interatomic distance of 2.05 Å, which was shown as the $[Ni(H_2O)_6]_2^+$ octahedral structures [48]. By contrast, $Ni(OH)_2$(s) showed a distinct frequency in both k^3-weighted and FT spectra because of the backscatter of the higher atomic coordination shell of Ni. The first-shell of $Ni(OH)_2$(s) was fitted by 5.8 O at 2.01 Å, whereas the second shell can be fitted by the Ni-Ni shell with ~ 6 Ni atoms at 3.10 Å (Table S3), consistent with previous reports [30, 49]. Although all sorption samples in the FT spectra contained a first-shell peak similar to the Ni(II)(aq) reference, the additional structural feature between 2.0-3.5 Å demonstrated the contribution of other atomic shells beyond the first O shell. For samples at pH 5.5 and 7.0, the FT peaks between 2.1 and 2.6 Å could provide evidence for a change in the local coordination structure of adsorbed Ni(II) relative to Ni(II)(aq) (Fig. 6B). Combined with the analysis of the XPS and FTIR data, the distinct structural feature might result from the coordination of Ni(II) with the carboxylate groups (i.e., Ni(II) coordinated with one of the oxygen atoms of the carboxylate group in a monodentate configuration). An attempt was made to fit the features using Ni-C single-scattering paths, but this attempt proved unsuccessful because the peak was too small to be distinguished from background spectral noise. The difficulty of fitting the Ni-C shell had been reported because the back-scattering of C atoms was weak and similar to O atoms owing to the low atomic number [20, 50]. For samples at pH 7.0, a split of the oscillation between 7.0 and 8.5 $Å^{-1}$ was observed for the sorption sample in the k^3-weighted spectrum, suggesting that $Ni(OH)_2$(s) was present, but not predominant. For the sample at pH 9.5, the pronounced FT feature at 5-8 Å was attributed to the back-scattering of adsorbed Ni(II) atoms in the local coordination environment [30, 51]. Correspondingly, the peak at 2.7 Å in the FT spectra can be well fitted by the Ni-Ni shell at 3.07 Å, indicating that the high-level sorption of Ni(II) on CNFs at pH 9.5 can be ascribed to surface precipitation. The results from EXAFS analysis proved that the inner-sphere surface complexation dominated the Ni(II) sorption on CNFs at approximately neutral pH, whereas the predominant contribution of Ni(II) sorption on CNFs was surface precipitation at higher pH.

Conclusions

CNFs demonstrate to be promising adsorbents for the highly efficient enrichment of

heavy metals in multi-component conditions. CNFs exhibited a higher chemical affinity for Pb(II) compared to Cu(II) and Ni(II) in competitive sorption systems. Based on the batch experiment, spectroscopic analysis and SCMs, Pb(II), Cu(II) and Ni(II) were adsorbed on CNFs by forming inner-sphere surface complexes at approximately neutral pH, whereas surface contributed to heavy metal sorption on CNFs at alkaline pH. The competitive sorption of heavy metals on CNFs in multi-metal systems was mainly dependent on the concentration of the heavy metals and their chemical properties. These observations are useful for the development and optimization of a new adsorbent which promises to be widely applied in situ remediation of heavy metals in natural environments. The contents are crucial for the simultaneous removal of metal ions from wastewater.

Associated content

Supporting Information

Additional characterization of the CNFs. More details on the experimental method and results, and surface complexation modeling.

Notes

The authors declare no competing financial interests.

Acknowledgements

This research was supported by the National Natural Science Foundation of China (21225730, 91326202 and 91126020), the priority Academic program development of Jiangsu Higher Education Institutions, and the Collaborative Innovation Center of Radiation Medicine of Jiangsu Higher Education Institutions.

References

[1] A. Anjum, C. Seth, M. Datta, Removal of As^{3+} Using Chitosan-Montmorillonite Composite: Sorptive Equilibrium and Kinetics, Adsorpt. Sci. Technol. 31 (2013) 303-324.

[2] X. Guo, F. Chen, Removal of arsenic by bead cellulose loaded with iron oxyhydroxide from groundwater, Environ. Sci. Technol. 39 (2005) 6808-6818.

[3] J.B. Zimmerman, J.R. Mihelcic, Smith, James, Global stressors on water quality and quantity, Environ. Sci. Technol. 42 (2008) 4247-4254.

[4] P.X. Sheng, Y.P. Ting, J.P. Chen, L. Hong, Sorption of lead, copper, cadmium, zinc, and nickel by marine algal biomass: characterization of biosorptive capacity and investigation of mechanisms, J. Colloid Interf. Sci. 275 (2004) 131-141.

[5] B. Anna, M. Kleopas, S. Constantine, F. Anestis, B. Maria, Adsorption of Cd (II), Cu (II), Ni (II) and Pb (II) onto natural bentonite: study in mono-and multi-metal systems, Environ. Earth Sci. 73 (2015) 5435-5444.

[6] Y. Sun, Q. Wang, C. Chen, X. Tan, X. Wang, Interaction between Eu (III) and graphene oxide nanosheets investigated by batch and extended X-ray absorption fine structure spectroscopy and by modeling techniques, Environ. Sci. Technol. 46 (2012) 6020-6027.

[7] G.D. Sheng, S.T. Yang, J. Sheng, J. Hu, X.L. Tan, X.K. Wang, Macroscopic and Microscopic Investigation of Ni(II) Sequestration on Diatomite by Batch, XPS, and EXAFS Techniques, Environ. Sci. Technol. 45 (2011) 7718-7726.

[8] X.L. Tan, M. Fang, X.M. Ren, H.Y. Mei, D.D. Shao, X.K. Wang, Effect of Silicate on the Formation and Stability of Ni-Al LDH at the gamma-Al2O3 Surface, Environ. Sci. Technol. 49 (2015) 6363-6363.

[9] H.S. Qian, S.H. Yu, L.B. Luo, J.Y. Gong, L.F. Fei, X.M. Liu, Synthesis of uniform Te@Carbon-Rich composite nanocables with photoluminescence properties and Carbonaceous nanofibers by the hydrothermal carbonization of glucose, Chem. Mater. 18 (2006) 2102-2108.

[10] H.W. Liang, X. Cao, W.J. Zhang, H.T. Lin, F. Zhou, L.F. Chen, S.H. Yu, Robust and Highly Efficient Free-Standing Carbonaceous Nanofiber Membranes for Water

Purification, Adv. Funct. Mater. 21 (2011) 3851-3858.

[11] D. Zhang, K. Ryu, X. Liu, E. Polikarpov, J. Ly, M.E. Tompson, C. Zhou, Transparent, conductive, and flexible carbon nanotube films and their application in organic light-emitting diodes, Nano Lett. 6 (2006) 1880-1886.

[12] Y. Wang, G. Du, H. Liu, D. Liu, S. Qin, N. Wang, C. Hu, X. Tao, J. Jiao, J. Wang, Z.L. Wang, Nanostructured sheets of Ti-O nanobelts for gas sensing and antibacterial applications, Adv. Funct. Mater. 18 (2008) 1131-1137.

[13] K. Yoon, B.S. Hsiao, B. Chu, Functional nanofibers for environmental applications, J. Mater. Chem. 18 (2008) 5326-5334.

[14] H.W. Liang, L. Wang, P.Y. Chen, H.T. Lin, L.F. Chen, D. He, S.H. Yu, Carbonaceous nanofiber membranes for selective filtration and separation of nanoparticles, Adv. Mater. 22 (2010) 4691-4695.

[15] Z.-Y. Wu, C. Li, H.-W. Liang, Y.-N. Zhang, X. Wang, J.-F. Chen, S.-H. Yu, Carbon nanofiber aerogels for emergent cleanup of oil spillage and chemical leakage under harsh conditions, Sci. Rep. 4 (2014) 4079.

[16] D.A. Kulik, S.U. Aja, V.A. Sinitsyn, S.A. Wood, Acid-base surface chemistry and sorption of some lanthanides on K^+-saturated marblehead illite: II. A multisite-surface complexation modeling, Geochim. Cosmochim. Acta, 64 (2000) 195-213.

[17] C. Ding, W. Cheng, Y. Sun, X. Wang, Determination of chemical affinity of graphene oxide nanosheets with radionuclides investigated by macroscopic, spectroscopic and modeling techniques, Dalton Trans. 43 (2014) 3888-3896.

[18] Y. Sun, S. Yang, Y. Chen, C. Ding, W. Cheng, X. Wang, Adsorption and Desorption of U(VI) on Functionalized Graphene Oxides: A Combined Experimental and Theoretical Study, Environ. Sci. Technol. 49 (2015) 4255-4262.

[19] Y.B. Sun, J.X. Li, X.K. Wang, The retention of uranium and europium onto sepiolite investigated by macroscopic, spectroscopic and modeling techniques, Geochim. Cosmochim. Acta, 140 (2014) 621-643.

[20] T.J. Strathmann, S.C. Myneni, Speciation of aqueous Ni (II)-carboxylate and Ni (II)-fulvic acid solutions: Combined ATR-FTIR and XAFS analysis, Geochim. Cosmochim. Acta, 68 (2004) 3441-3458.

[21] Z. Reddad, C. Gerente, Y. Andres, P. Le Cloirec, Modeling of single and competitive metal adsorption onto a natural polysaccharide, Environ. Sci. Technol. 36 (2002) 2242-2248.

[22] X. Gu, L.J. Evans, S.J. Barabash, Modeling the adsorption of Cd (II), Cu (II), Ni (II), Pb (II) and Zn (II) onto montmorillonite, Geochim. Cosmochim. Acta, 74 (2010) 5718-5728.

[23] R.P. Deo, W. Songkasiri, B.E. Rittmann, D.T. Reed, Surface complexation of neptunium (V) onto whole cells and cell components of Shewanella alga: modeling and experimental study, Environ. Sci. Technol. 44 (2010) 4930-4935.

[24] H. S. Qian, S. H. Yu, J. Y. Gong, L. B. Luo, L. f. Fei, High-quality luminescent tellurium nanowires of several nanometers in diameter and high aspect ratio synthesized by a poly (vinyl pyrrolidone)-assisted hydrothermal process, Langmuir, 22 (2006) 3830-3835.

[25] W. Cheng, Z. Jin, C. Ding, M. Wang, Simultaneous sorption and reduction of U (vi) on magnetite–reduced graphene oxide composites investigated by macroscopic, spectroscopic and modeling techniques, Rsc Adv. 5 (2015) 59677-59685.

[26] A.K. Karamalidis, E.A. Voudrias, Anion leaching from refinery oily sludge and ash from incineration of oily sludge stabilized/solidified with cement. Part I. Experimental results, Environ. Sci. Technol. 42 (2008) 6116-6123.

[27] S. Goldberg, Use of surface complexation models in soil chemical systems, Adv. Agron, 47 (1992) 233-329.

[28] S. Goldberg, Constant capacitance model. Chemical surface complexation model for describing adsorption of toxic trace elements on soil minerals, in: ACS Symposium series-American Chemical Society (USA), 1993.

[29] A. Omoike, J. Chorover, Spectroscopic study of extracellular polymeric substances from Bacillus subtilis: Aqueous chemistry and adsorption effects, Biomacromolecules, 5 (2004) 1219-1230.

[30] S. Yang, G. Sheng, X. Tan, J. Hu, J. Du, G. Montavon, X. Wang, Determination of Ni (II) uptake mechanisms on mordenite surfaces: a combined macroscopic and microscopic approach, Geochim. Cosmochim. Acta, 75 (2011) 6520-6534.

[31] T. Rabung, M. Pierret, A. Bauer, H. Geckeis, M. Bradbury, B. Baeyens, Sorption of Eu (III)/Cm (III) on Ca-montmorillonite and Na-illite. Part 1: Batch sorption and time-resolved laser fluorescence spectroscopy experiments, Geochim. Cosmochim. Acta, 69 (2005) 5393-5402.

[32] V. Sinitsyn, S. Aja, D. Kulik, S. Wood, Acid–base surface chemistry and sorption of some lanthanides on K^+-saturated Marblehead illite: I. results of an experimental investigation, Geochim. Cosmochim. Acta, 64 (2000) 185-194.

[33] P.X. Sheng, Y. P. Ting, J.P. Chen, Biosorption of heavy metal ions (Pb, Cu, and Cd) from aqueous solutions by the marine alga Sargassum sp. in single-and multiple-metal systems, Ind. Eng. Chem. Res. 46 (2007) 2438-2444.

[34] D.C.W. Tsang, I.M.C. Lo, Competitive Cu and Cd sorption and transport in soils: A combined batch kinetics, column, and sequential extraction study, Environ. Sci. Technol. 40 (2006) 6655-6661.

[35] B. Xiao, K.M. Thomas, Competitive adsorption of aqueous metal ions on an oxidized nanoporous activated carbon, Langmuir, 20 (2004) 4566-4578.

[36] A.C. Scheinost, S. Abend, K.I. Pandya, D.L. Sparks, Kinetic controls on Cu and Pb sorption by ferrihydrite, Environ. Sci. Technol. 35 (2001) 1090-1096.

[37] A.S. Gunasekara, B. Xing, Sorption and desorption of naphthalene by soil organic matter, J. environ. qual. 32 (2003) 240-246.

[38] T. Undabeytia, S. Nir, G. Rytwo, C. Serban, E. Morillo, C. Maqueda, Modeling adsorption-desorption processes of Cu on edge and planar sites of montmorillonite, Environ. Sci. Technol. 36 (2002) 2677-2683.

[39] W. Um, C. Papelis, Metal ion sorption and desorption on zeolitized tuffs from the Nevada Test Site, Environ. Sci. Technol. 38 (2004) 496-502.

[40] [7] W. Wu, W. Jiang, W. Zhang, D. Lin, K. Yang, Influence of functional groups on desorption of organic compounds from carbon nanotubes into water: insight into desorption hysteresis, Environ. Sci. Technol. 47 (2013) 8373-8382.

[41] C. Ding, W. Cheng, Y. Sun, X. Wang, Effects of Bacillus subtilis on the reduction of U (VI) by nano-Fe 0, Geochim. Cosmochim. Acta, 165 (2015) 86-107.

[42] C.C. Ding, S. Feng, X.L. Li, J.L. Liao, Y.Y. Yang, Z. An, Q.Q. Wu, D. Zhang, J.J.

Yang, J. Tang, J. Zhang, N. Liu, Mechanism of thorium biosorption by the cells of the soil fungal isolate Geotrichum sp dwc-1, Radiochim. Acta, 102 (2014) 175-184.

[43] J.M. Gong, T. Liu, X.Q. Wang, X.L. Hu, L.Z. Zhang, Efficient Removal of Heavy Metal Ions from Aqueous Systems with the Assembly of Anisotropic Layered Double Hydroxide Nanocrystals@Carbon Nanosphere, Environ. Sci. Technol. 45 (2011) 6181-6187.

[44] Y. Sun, D. Shao, C. Chen, S. Yang, X. Wang, Highly efficient enrichment of radionuclides on graphene oxide-supported polyaniline, Environ. Sci. Technol. 47 (2013) 9904-9910.

[45] C. Ding, W. Cheng, Y. Sun, X. Wang, Novel fungus-Fe3O4 bio-nanocomposites as high performance adsorbents for the removal of radionuclides, J. Hazard. Mater. 295 (2015) 127-137.

[46] X.Y. Gu, L.J. Evans, Surface complexation modelling of Cd(II), Cu(II), Ni(II), Pb(II) and Zn(II) adsorption onto kaolinite, Geochim. Cosmochim. Acta, 72 (2008) 267-276.

[47] G. Sheng, L. Ye, Y. Li, H. Dong, H. Li, X. Gao, Y. Huang, EXAFS study of the interfacial interaction of nickel (II) on titanate nanotubes: Role of contact time, pH and humic substances, Chem. Eng. J. 248 (2014) 71-78.

[48] J.-F. Groust, C. Pommier, L. Stievano, F. Villain, C. Giorgetti, F. Baudelet, P. Massiani, Real time monitoring of the evolution of Ni2+ environment in faujasite upon rehydration by in situ dispersive-EXAFS, Catal. Lett. 102 (2005) 257-260.

[49] X. Ren, S. Yang, F. Hu, B. He, J. Xu, X. Tan, X. Wang, Microscopic level investigation of Ni (II) sorption on Na-rectorite by EXAFS technique combined with statistical F-tests, J. Hazard. Mater. 252 (2013) 2-10.

[50] T.J. Strathmann, S.C. Myneni, Effect of soil fulvic acid on nickel (II) sorption and bonding at the aqueous-boehmite (γ-AlOOH) interface, Environ. Sci. Technol. 39 (2005) 4027-4034.

[51] A.M. Scheidegger, E. Wieland, A.C. Scheinost, R. Dähn, P. Spieler, Spectroscopic evidence for the formation of layered Ni-Al double hydroxides in cement, Environ. Sci. Technol. 34 (2000) 4545-4548.

Figure captions

Fig. 1. The characterization of CNFs, A and B: SEM and high resolution TEM images, respectively; C: high resolution of C 1s XPS spectrum; D: potentiometric acid-base titration data in the presence of 0.001 M $NaClO_4$.

Fig. 2. Effect of pH on individual Pb(II) (A), Cu(II) (B) and Ni(II) (C) on CNFs in 0.001, 0.01 and 0.1 mol/L $NaClO_4$; D: competitive sorption of heavy metals in ternary Pb-Cu-Ni system in 0.001 mol/L $NaClO_4$; Solid lines: CCM model fits in 0.001 mol/L $NaClO_4$ and the corresponding surface species; C_0 = 0.2 mmol/L, m/V = 0.20 g/L, T = 25 ± 1°C.

Fig. 3. Sorption isotherms for heavy metals on CNFs in single- and binary/ternary-metal systems, A: Ni(II), B: Cu(II), C: Pb(II); desorption of heavy metal from CNFs, D: Ni(II), E: Cu(II), F: Pb(II); pH = 5.5 ± 0.2, m/V = 0.20 g/L, T = 25 ± 1°C, I = 0.001 mol/L.

Fig. 4. FTIR spectra of CNFs before and after heavy metal sorption; C_0 = 0.2 mmol/L, pH = 5.5 ± 0.2, m/V = 0.20 g/L, T = 25 ± 1 °C, I = 0.001 mol/L.

Fig. 5. Total scans of XPS spectra (A) and the high-resolution O 1s spectra (B)of CNFs and CNFs after sorption; C_0 = 0.2 mmol/L, pH = 5.5 ± 0.2, m/V = 0.20 g/L, T = 25 ± 1°C, I = 0.001 mol/L.

Fig. 6. k^3-weighted Ni K-edge EXAFS spectra (A) and the corresponding Fourier transforms (B) of the reference samples and selected sorption samples at pH 5.5, 7.0 and 9.5; Solid lines: EXAFS results, dashed lines: fitting results; C_0 = 0.2 mmol/L, m/V = 0.20 g/L, T = 25 ± 1°C, I = 0.001 mol/L.

Figures

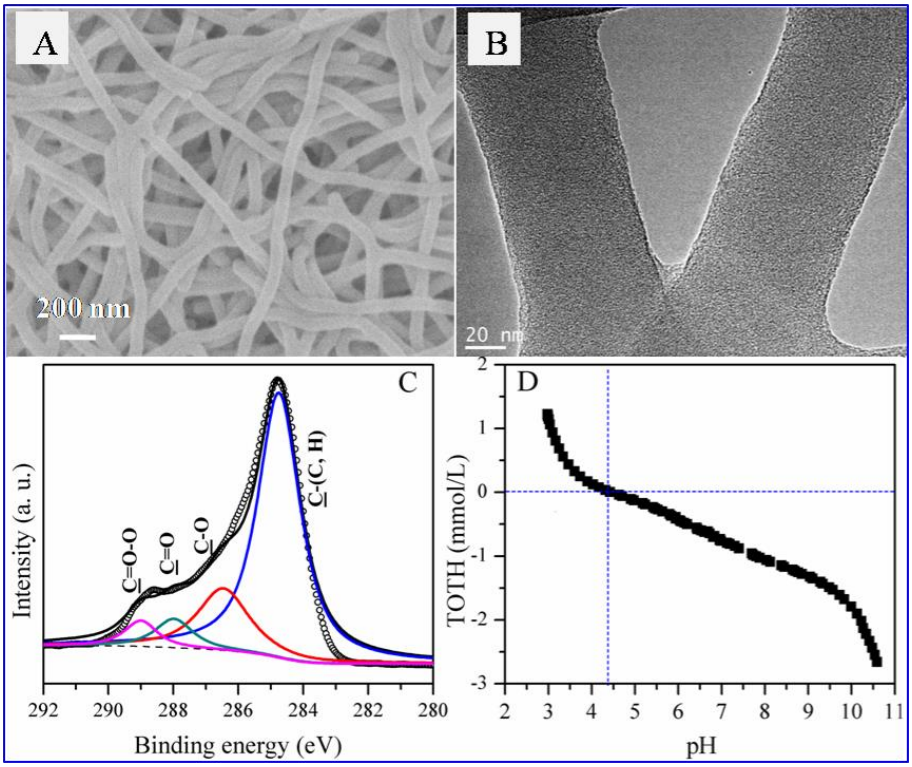

Fig. 1

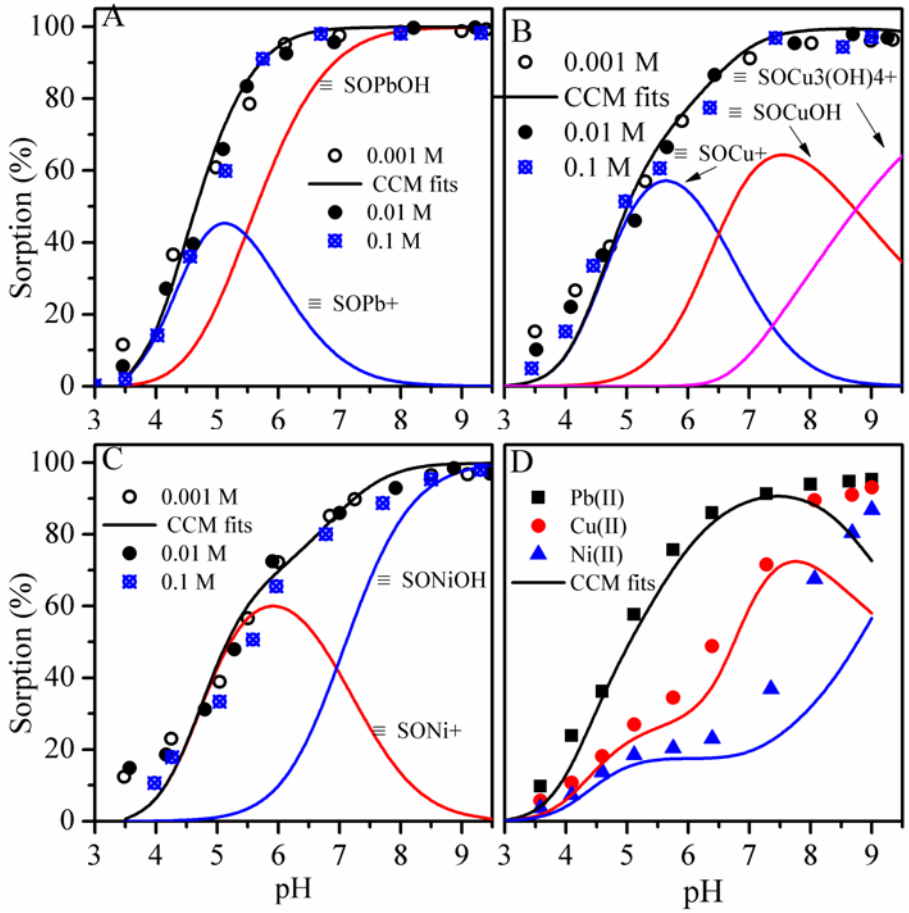

Fig. 2

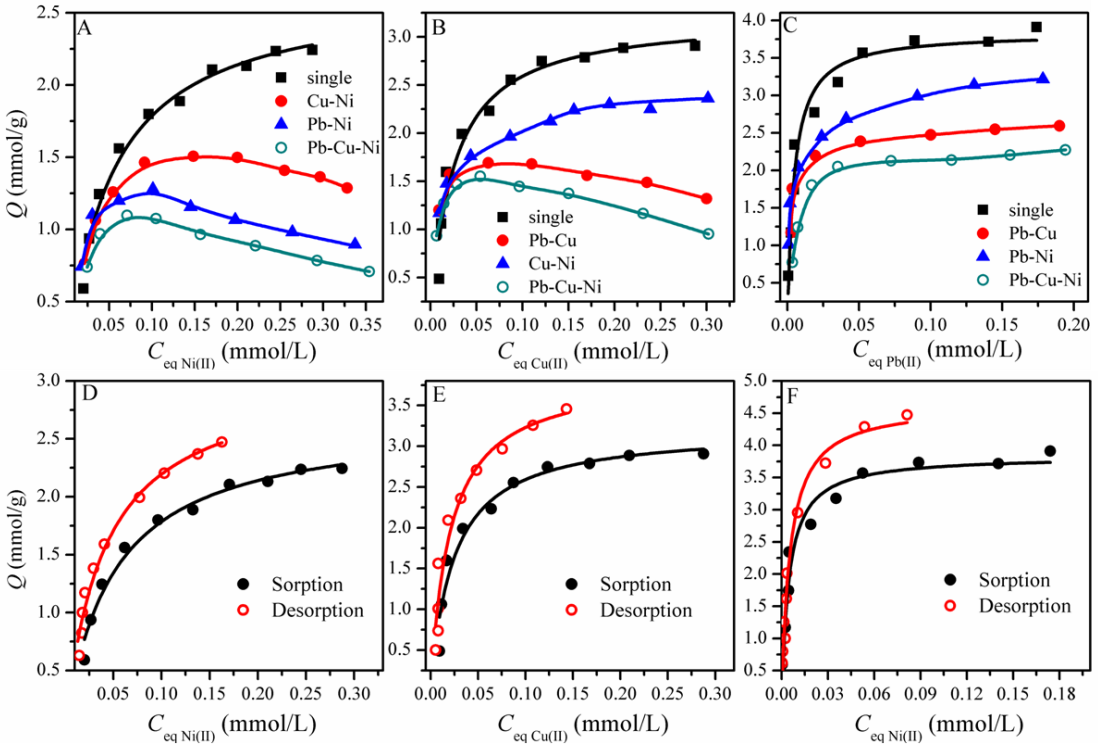

Fig. 3

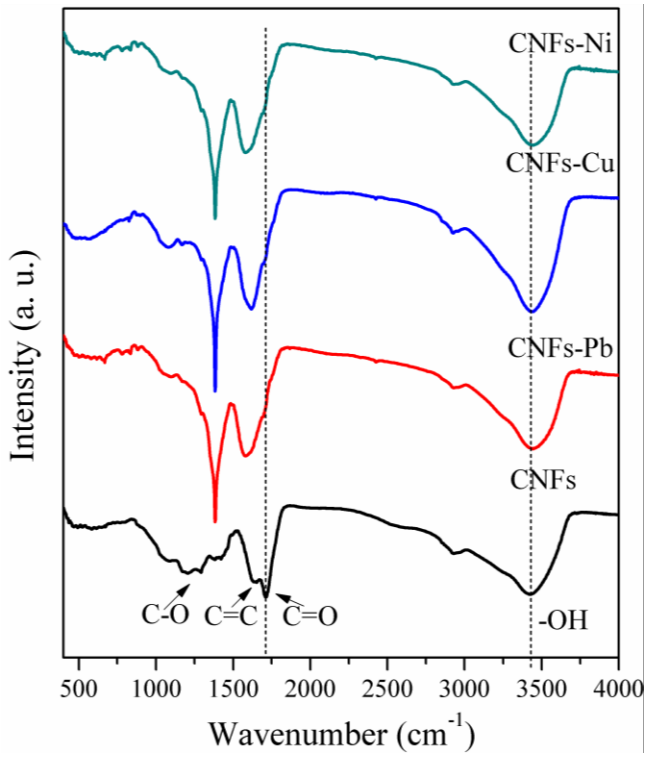

Fig. 4

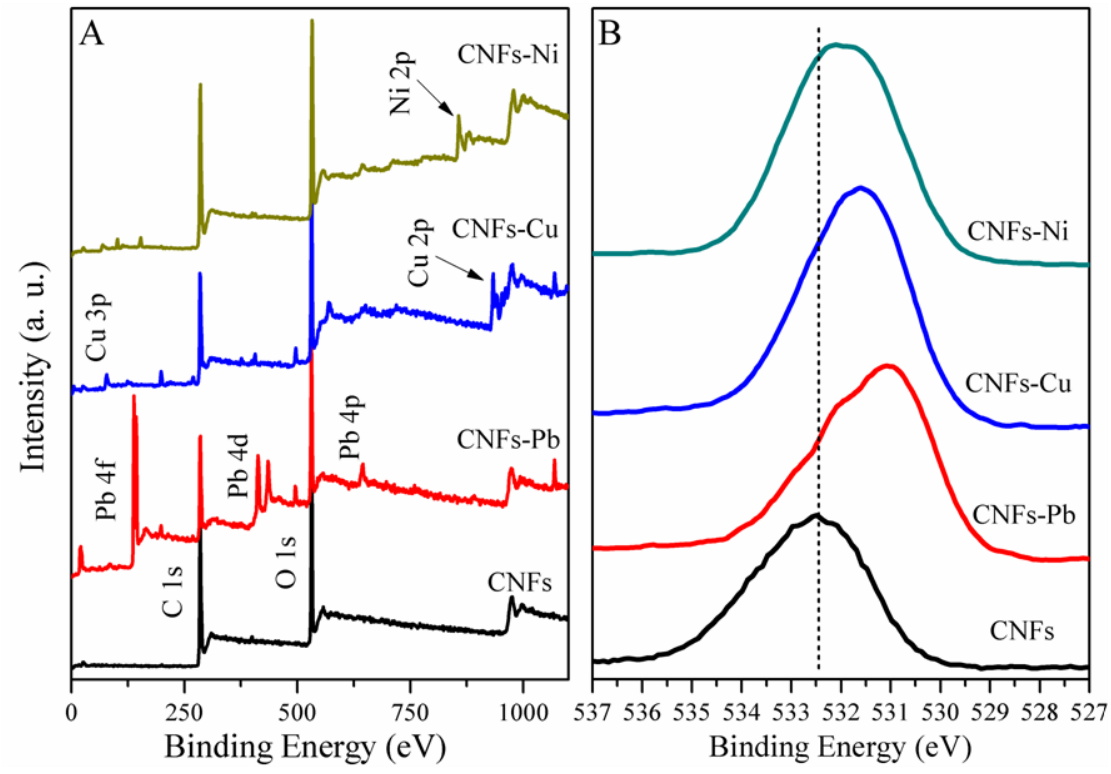

Fig. 5

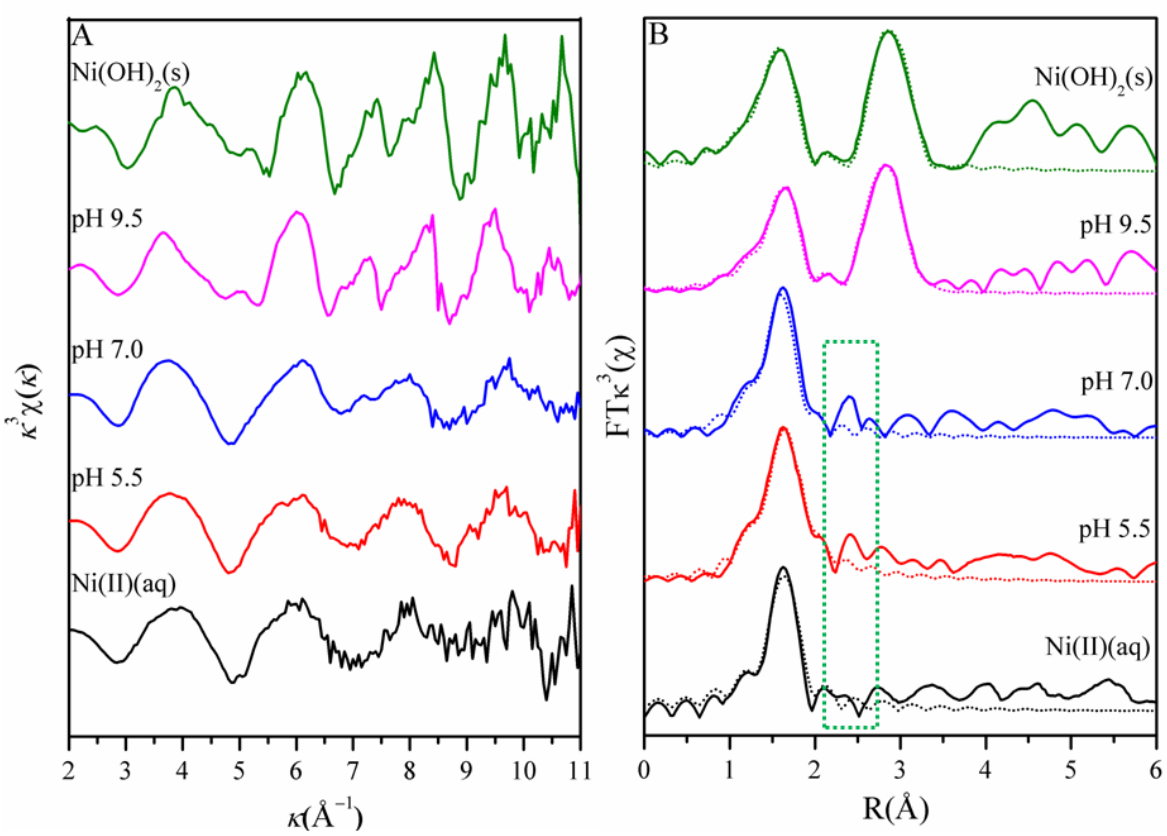

Fig. 6

Table 1. Parameters for the fitting of the sorption of heavy metals on CNFs.

S_{BET} ($m^2 \cdot g^{-1}$)		150.30		
Surface site density ($sites \cdot nm^{-2}$)		17.25[a]		
Specific capacitance ($F \cdot m^{-2}$)		2.01[b]		
Surface acidity constants (log K^0)		$\equiv SOH + H^+ \leftrightarrow \equiv SOH_2^+$		4.40 [a]
		$\equiv SOH \leftrightarrow \equiv SO^- + H^+$		-4.75 [a]
Metal species		sorption constants (log K)		
		$\equiv SOM^+$	≡SOMOH	$\equiv SOM_3(OH)_4^-$
Pb(II)		-0.45(4)	-5.90(3)	
Cu(II)		-0.79(3)	-7.10(4)	-19.50(5)
Ni(II)		-0.96(5)	-7.70(5)	

[a] Obtained by potentiometric titrations; [b] value from Goldberg [28]

Table 2. Langmuir constants for the sorption of Pb(II), Cu(II), and Ni(II) on CNFs in the absence and presence competing ions.

species	Pb(II)			Cu(II)			Ni(II)		
Competing ions[a]	-	Cu(II)	Ni(II)	-	Pb(II)	Ni(II)	-	Pb(II)	Cu(II)
Q_{max} (mmol/g)	3.84	2.90	3.38	3.21	2.03	2.86	2.67	1.75	2.14
Q_{max} (mg/g)	795.65	600.88	700.34	204.00	129.01	181.75	156.70	102.71	125.60
b (L/mmol)	212.31	208.78	178.89	41.70	39.13	38.16	20.22	30.75	25.35
b (L/mg)	1.02	1.01	0.86	0.66	0.62	0.60	0.34	0.52	0.43
R^2	0.96	0.98	0.98	0.95	0.96	0.97	0.98	0.99	0.98

[a] Initial concentration of competing ions was 0.2 mmol/L

Table 3. The maximum sorption capacities (mmol/g)/ (mg/g)[a] of Pb(II), Cu(II), and Ni(II) on CNFs in binary-metal and ternary-metal systems from the experimental data.

System	Pb(II)	Cu(II)	Ni(II)
Pb-Cu	2.60/ 538.72	1.70/ 108.04	
Pb-Ni	3.21/ 665.11		1.28/ 75.12
Cu-Ni		2.36/ 149.98	1.51/ 88.62
Pb-Cu-Ni	2.27/ 470.34	1.55/ 98.50	1.1/ 64.56

[a] Expressed in units of mmol/g or mg/g.